

1 **Quantitative benzimidazole resistance and fitness effects of parasitic nematode**
2 **beta-tubulin alleles**

3

4 Clayton M. Dilks^{a,b}, Steffen R. Hahnel^{a,*}, Qicong Sheng^a, Lijiang Long^{c,d}, Patrick T.
5 McGrath^c, Erik C. Andersen^{a,b,‡}

6

7 ^aMolecular Biosciences, Northwestern University, Evanston, IL 60208

8 ^bInterdisciplinary Biological Sciences Program, Northwestern University, Evanston, IL
9 60208

10 ^cCenter for Biological Sciences, Georgia Institute of Technology, Atlanta, GA, 30332 USA

11 ^dInterdisciplinary Graduate Program in Quantitative Biosciences, Georgia Institute of
12 Technology, Atlanta, GA, 30332 USA

13

14

15 **Keywords:** anthelmintic resistance, *C. elegans*, competitive fitness effects, high-
16 throughput assays, benzimidazoles

17

18 **‡Corresponding Author:**

19 Erik C. Andersen, Ph.D.

20 Department of Molecular Biosciences

21 Northwestern University

22 **4619 Silverman Hall**

23 2205 Tech Drive

24 Evanston, IL 60208

25 847-467-4382

26 erik.andersen@northwestern.edu

27

28 Clay: 0000-0002-4622-8460

29 Patrick: 0000-0002-1598-3746

30 Erik: 0000-0003-0229-9651

31

32 **Highlights**

33

34 • All three canonical parasitic nematode beta-tubulin alleles (F167Y, E198A, F200Y)
35 and two newly identified alleles (E198V, E198L) confer equal levels of benzimidazole
36 resistance in a defined genetic background using single-generation, high-replication drug
37 response assays.

38 • Beta-tubulin variants are strongly selected in albendazole conditions in
39 multigenerational competitive fitness assays, but these alleles confer different levels of
40 benzimidazole resistance over time.

41 • Only the E198V allele confers a fitness cost in control (non-benzimidazole)
42 conditions as compared to all other tested beta-tubulin alleles, suggesting that this
43 intermediate allele might only be found in field populations at low frequency because it
44 causes reduced fitness.

45

46

47

48 **Present address**

49 *Bayer Animal Health, Leverkusen, Germany

50

51

52

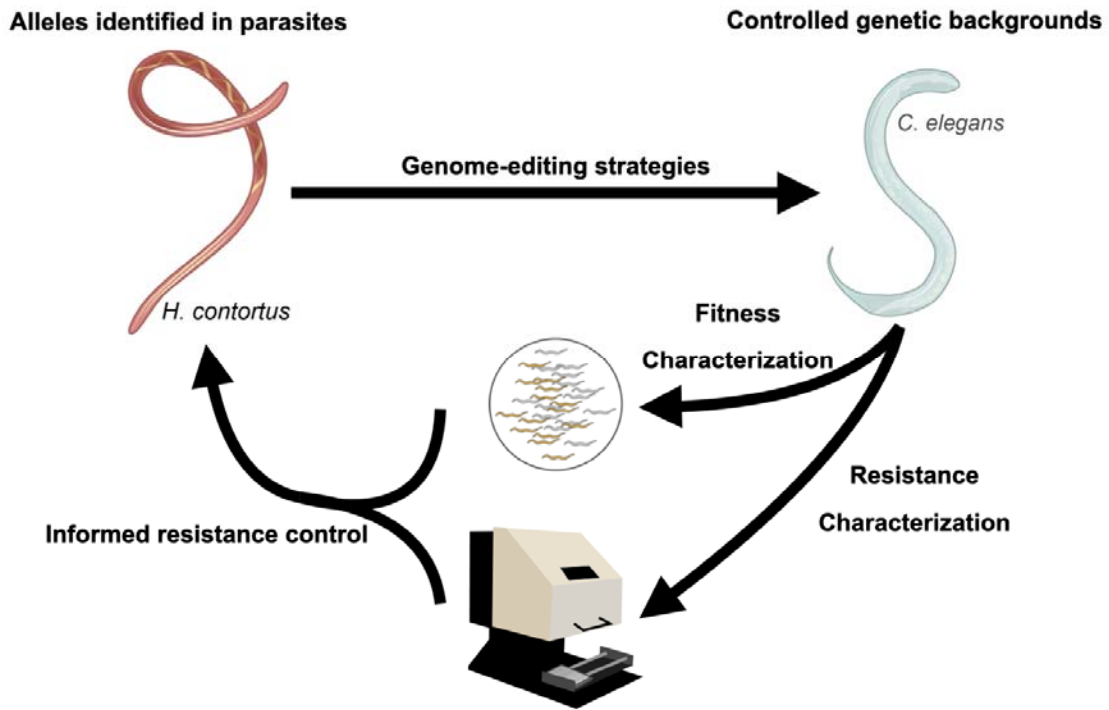
53

54 **Abstract**

55 Infections by parasitic nematodes inflict a huge burden on the health of humans and
56 livestock throughout the world. Anthelmintic drugs are the first line of defense against
57 these infections. Unfortunately, resistance to these drugs is rampant and continues to
58 spread. To improve treatment strategies, we must understand the genetics and molecular
59 mechanisms that underlie resistance. Studies of the fungus *Aspergillus nidulans* and the
60 free-living nematode *Caenorhabditis elegans* discovered that a beta-tubulin gene is
61 mutated in benzimidazole (BZ) resistant strains. In parasitic nematode populations, three
62 canonical beta-tubulin alleles, F200Y, E198A, and F167Y, have long been correlated with
63 resistance. Additionally, improvements in sequencing technologies have identified new
64 alleles - E198V, E198L, E198K, E198I, and E198Stop - also correlated with BZ resistance.
65 However, none of these alleles have been proven to cause resistance. To empirically
66 demonstrate this point, we independently introduced the three canonical alleles as well as
67 two of the newly identified alleles, E198V and E198L, into the BZ susceptible *C. elegans*
68 N2 genetic background. These genome-edited strains were exposed to both albendazole
69 and fenbendazole to quantitatively measure animal responses to BZs. We used a range of
70 doses for each BZ compound to define response curves and found that all five of the
71 alleles conferred resistance to BZ compounds equal to a loss of the entire beta-tubulin
72 gene. These results prove that the parasite beta-tubulin alleles cause resistance. The
73 E198V allele is found at low frequencies in natural parasite populations, suggesting that it
74 could affect fitness. We performed competitive fitness assays and demonstrated that the
75 E198V allele reduces animal health, supporting the hypothesis that this allele is less fit in
76 field populations. Overall, we present a powerful platform to quantitatively assess
77 anthelmintic resistance and effects of specific resistance alleles on organismal fitness in
78 the presence or absence of the drug.

80 **Graphical Abstract**

81



82

83

84

85

86 **1. Introduction**

87 Parasitic nematode infections cause a major health and economic burden that
88 impacts billions of people around the globe (Hotez et al., 2014; Lustigman et al., 2012). In
89 animal health, parasite infections lead to major reductions in livestock yields (Charlier et
90 al., 2009; Kahn and Woodgate, 2012; Sutherland and Leathwick, 2011). Anthelmintics are
91 the main defense against parasitic nematode infections, but an alarmingly low number of
92 drug classes are both efficacious and safe (Kaplan and Vidyashankar, 2012). The four
93 most commonly used classes of anthelmintics are the benzimidazoles (BZs), macrocyclic
94 lactones (MLs), nicotinic acetylcholine receptor agonists (NACHA), and amino-acetonitrile
95 derivatives (AADs). The first BZ was developed and implemented in veterinary medicine in
96 1962 under the name thiabendazole (Campbell and Cuckler, 1962; Merck and Sharp &
97 Dohme Research Laboratories. Animal Science Research, 1962). Large-scale adoption
98 and blanket usage of this drug placed a strong active pressure on parasites and quickly
99 caused resistant populations throughout the world (Theodorides et al., 1970). Today,
100 resistance to the two most widely used BZs, albendazole and fenbendazole, is common
101 and found globally (Kaplan and Vidyashankar, 2012).

102 The genes that underlie resistance can be used to inform parasitic nematode
103 control practices by monitoring the spread of resistance alleles in parasite populations.
104 The alleles present in a population can predict drug efficacy and enable the maintenance
105 of sensitive refugia populations (Hodgkinson et al., 2019; Muchiut et al., 2018). For BZ
106 compounds, the first resistance gene, encoding a beta-tubulin, was identified in studies of
107 the fungus *Aspergillus nidulans* (Hastie and Georgopoulos, 1971; Sheir-Neiss et al.,
108 1978). Subsequently, *Caenorhabditis elegans* BZ selection experiments isolated resistant
109 strains with mutations in a nematode-specific beta-tubulin gene, *ben-1* (Driscoll et al.,
110 1989). This connection between beta-tubulin and nematode BZ resistance led to the
111 discovery of mutations in *ben-1* homologs in BZ resistant parasitic nematode populations

112 (Roos et al., 1990). The first allele in a *ben-1* homolog (*Hco-tub8-9*) that was correlated
113 with BZ resistance in *Haemonchus contortus* populations was F200Y (Kwa et al., 1993,
114 1994). Subsequent surveys of resistant *H. contortus* populations identified two additional
115 alleles correlated with resistance, F167Y (Silvestre and Cabaret, 2002) and E198A (Ghisi
116 et al., 2007). These three putative resistance alleles are considered canonical because
117 they are commonly found in resistant populations (Avramenko et al., 2019; Hinney et al.,
118 2020; Redman et al., 2015). Recently, improved nematode genotyping techniques have
119 enabled the detection of additional mutations at the 198 position: E198V, E198L, E198K,
120 E198I, and E198Stop (Avramenko et al., 2019; Mohammedsalih et al., 2020; Redman et
121 al., 2015; von Samson-Himmelstjerna et al., 2009). These beta-tubulin alleles represent
122 promising markers of BZ resistance across parasitic nematode populations.

123 However, parasitic nematode studies have only correlated beta-tubulin alleles with
124 BZ resistance. To go beyond correlation, a causal relationship between beta-tubulin and
125 BZ resistance must be defined, which is difficult, if not impossible, in parasitic nematode
126 species because genome-editing and characterized genetic backgrounds are required.
127 Causal relationships between genes and phenotypes require empirical tests of sufficiency
128 and necessity. To show that the beta-tubulin gene is sufficient for BZ response, functional
129 replacement of the mutated gene must be shown to confer BZ sensitivity. This experiment
130 was performed previously using overexpression of *C. elegans ben-1* or *H. contortus tub8-*
131 *9* (Kwa et al., 1995). To show that beta-tubulin is necessary for BZ response, only the
132 beta-tubulin gene must be mutated in a defined genetic background and shown to cause
133 BZ resistance. Recently, the F167Y and F200Y alleles were shown to confer BZ
134 resistance in *C. elegans* in a controlled genetic background (Hahnel et al., 2018; Kitchen
135 et al., 2019).

136 Recent results indicate that BZ resistance is heterogeneous (Crook et al., 2016;
137 Howell et al., 2008). Population-wide sequencing of beta-tubulin alleles have found

138 different alleles in the same population (Avramenko et al., 2019; Hinney et al., 2020;
139 Mohammedsalih et al., 2020; Redman et al., 2015; von Samson-Himmelstjerna et al.,
140 2009). The frequency of each allele likely is determined both by its level of resistance and
141 its effect on growth. Field observations have shown that populations maintain resistance
142 after BZ pressure is removed (van Wyk et al., 1997), which suggests that they do not
143 cause decreases in fitness. Measurements of the exact levels of resistance and any
144 growth effects associated with the alleles are nearly impossible in field populations, so
145 controlled laboratory experiments are required to test these hypotheses. In *C. elegans*, the
146 F200Y and a loss-of-function *ben-1* allele conferred strong BZ resistance but no growth
147 consequences compared to a wild-type control strain in conditions that lacked BZ (Hahnel
148 et al., 2018), suggesting that the maintenance of resistance is not a detriment to fitness.
149 One untested hypothesis of a possible interplay between resistance and fitness
150 consequences was observed at the 198 position. The E198V allele has been detected at
151 low frequencies in populations that also harbor the E198L allele (Avramenko et al., 2019;
152 Mohammedsalih et al., 2020), suggesting that the E198V allele (**Supplemental Fig. 1**)
153 confers lower levels of resistance and/or has a fitness detriment. In *C. elegans*, this
154 interplay between resistance and fitness consequences can be determined using a
155 defined genetic background, genome editing, and competitive fitness assays.

156 Here, we introduced beta-tubulin alleles from parasitic nematodes into a BZ-
157 susceptible *C. elegans* laboratory strain using the CRISPR-Cas9 system. Independently
158 generated alleles were assayed using multiple high-throughput techniques to determine
159 levels of resistance and effects on fitness in both albendazole and fenbendazole. We
160 definitively demonstrated that the beta-tubulin alleles from parasitic nematodes confer
161 equivalent levels of BZ resistance. Additionally, we quantitatively assessed effects on
162 competitive fitness in both control and BZ conditions. All parasite beta-tubulin alleles
163 conferred BZ resistance as shown by an increase in allele frequency when competed

164 against a wild-type control strain. In control conditions, each parasite beta-tubulin allele
165 grew as well as a wild-type control strain, except for the fitness detriment conferred by the
166 E198V allele. These results offer an explanation for why some alleles are found at higher
167 frequencies and why the E198V allele is only found at low frequencies in parasite
168 populations.

169

170

171

172

173

174

175

176

177

178

179

180

181

182

183

184

185

186

187

188

189

190

191 **2. Methods**

192

193 **2.1 *C. elegans* strains**

194 Animals in this study were grown at 20°C on modified nematode growth medium
195 (NGMA) that contains 1% agar and 0.7% agarose seeded with OP50 bacteria (Andersen
196 et al., 2014). For each assay, strains were grown for three generations following starvation
197 in an attempt to reduce the multigenerational effects of starvation (Andersen et al., 2014).
198 The existing strains harboring the *ben-1* deletion allele (*ean64*) or the F200Y alleles
199 (*ean100*, *ean101*) (Hahnel et al., 2018) were used as controls for all experiments in this
200 study. The barcoded wild-type control strain PTM229 *dpy-10(kah81)* was used in
201 competitive fitness assays (Zhao et al., 2018). All strains in this study (Supplemental Table
202 1) were generated in the N2 genetic background with modifications introduced using the
203 CRISPR-Cas9 genome-editing system as described previously (Hahnel et al., 2018).

204

205 **2.2 CRISPR-Cas9 genome editing**

206 All edited *ben-1* strains were generated in the N2 genetic background using
207 CRISPR-Cas9-mediated genome editing. Targeted genome editing was facilitated using a
208 co-CRISPR strategy (described below) to increase the chance of discovering successful
209 edits (Kim et al., 2014). For the *ben-1* E198A, F167Y, E198V, and E198L allele
210 replacement strains, we designed sgRNAs that targeted the *ben-1* locus and the *dpy-10*
211 locus using the CRISPR design tool on the online analysis platform Benchling
212 (www.benchling.com). These sgRNAs were ordered from Synthego (Redwood City, CA)
213 and injected at 5 µM for the *ben-1* sgRNA and 1 µM for the *dpy-10* sgRNA. Single-
214 stranded oligodeoxynucleotides (ssODN) templates for homology-directed repair (HDR)
215 for both the *ben-1* and *dpy-10* alleles were ordered as ultramers (IDT, Skokie, IL) and

216 injected at final concentrations of 6 μ M and 0.5 μ M, respectively. Cas9 protein (IDT,
217 Skokie, IL) was also included and injected at a final concentration of 5 μ M and incubated
218 with the previously described sgRNAs and ssODNs at room temperature for one hour prior
219 to injection. After incubation, the mixture was injected into the germlines of young adult
220 hermaphrodite animals. These animals were singled to fresh 6 cm NGMA plates 18 hours
221 post-injection. After 48 hours, F1 progeny were screened for animals with the Rol
222 phenotype, and the individuals that displayed the Rol phenotype were singled onto new 6
223 cm NGMA plates and allowed to lay offspring. For the *ben-1* allele replacements, ssODN
224 templates contained the desired nucleotide edit and a synonymous edit in the PAM site to
225 prevent repeated cleavage by the sgRNA:Cas9 complex post introduction of the edit. In
226 addition to preventing repeated cleavage at the PAM site, this edit introduced a new
227 restriction site into the sequence. The E198A and E198V repair ssODNs introduced a
228 *BtsCI* restriction site, the E198L repair ssODN introduced a *Hpy188I* restriction site, and
229 F167Y introduced a *SacI* cut site. Following PCR of the edited region, the PCR products
230 were incubated with the restriction enzyme (New England Biolabs, Ipswich, MA) that had a
231 recognition site introduced in the repair oligonucleotide for the desired edit. Successful
232 edits were identified by an altered restriction pattern. F2 non-Rol individuals from parents
233 with successful edits were placed on single plates to generate homozygous progeny. F2
234 individuals were then genotyped following the same process described above, and
235 successful edits were Sanger sequenced to ensure homozygosity of the desired edits
236 before use in future experiments. Independent edits of each allele were generated to
237 control for off-target effects of the CRISPR-Cas9 process. All oligonucleotides used in this
238 study are available upon request (Supplemental Table 2).

239

240 **2.3 High-throughput fitness assays**

241 High-throughput fitness assays were performed as previously described (Evans
242 and Andersen, 2020; Zdraljevic et al., 2017). Briefly, a 0.5 cm³ NGMA piece was cut from
243 a plate containing starved individuals to a new NGMA plate. Two days later, gravid
244 hermaphrodites from the new NGMA plate were placed into a bleach solution on a 6 cm
245 agar plate to clean and synchronize each strain. The next day, five L1 larvae were moved
246 to 6 cm NGM plates and allowed to reproduce over the course of five days until the
247 offspring had reached the L4 larval stage. Five L4 individuals were transferred to new 6
248 cm NGMA plates and allowed to grow and reproduce for four days. After this growth,
249 strains were bleach synchronized to generate a large pool of synchronized unhatched
250 embryos for each strain. These embryos were diluted to roughly one embryo per μL in K
251 medium (Boyd et al., 2012). Embryos were placed into 96-well plates at roughly 50
252 embryos per well in 50 μL of K medium and allowed to hatch overnight. The next morning,
253 a mixture HB101 lysate (García-González et al., 2017) at a concentration of 5 mg/mL and
254 either drug (albendazole or fenbendazole) in DMSO or DMSO alone was added to the
255 solution. Final DMSO concentrations were kept at 1% for all doses and experiments. For
256 dose response assays, drugs were used at 0, 6.25, 12.5, 25, 50, and 100 μM . For high-
257 replication albendazole and fenbendazole assays, both drugs were used at a final
258 concentration of 30 μM because at this concentration N2 showed a severe developmental
259 delay and the parasite beta-tubulin alleles had begun to be developmentally delayed in
260 dose response experiments. After 48 hours of growth in either control or BZ conditions,
261 animals were scored using the COPAS BIOSORT (Union Biometrica, Holliston MA) after
262 treatment with sodium azide at 50 mM to straighten the animals (Brady et al., 2019;
263 Hahnel et al., 2018; Zdraljevic et al., 2017). Animal optical density integrated by the animal
264 length (EXT) was measured with the COPAS BIOSORT for each individual. The median
265 optical density (median.EXT) of nematode populations in each well was used for
266 quantitative BZ responses.

267

268 **2.4 Optical density trait processing**

269 All growth trait processing and analyses were completed using the R(3.6.1)
270 package *easysorter* (Shimko and Andersen, 2014) with the `v3_assay = TRUE` argument
271 added to the *sumplate* function. Beyond modifications for changes in the assay workflow,
272 analyses were performed as described previously (Hahnel et al., 2018) for high-replication
273 single-concentration experiments. For dose-response experiments, phenotypes for each
274 strain were normalized to the value of each strain in control conditions (1% DMSO). For
275 normalization, we calculated the mean of our trait of interest (`median.EXT`) in control
276 conditions and subtracted that value from the phenotypic values from each of the different
277 doses. This normalization was performed on a strain-specific basis to control for any
278 differences in the starting populations among strains.

279

280 **2.5 Competition assays**

281 We used previously established pairwise competition assays to assess organismal
282 fitness (Zhao et al., 2018). The fitness of a strain is determined by comparing the allele
283 frequency of a strain against the allele frequency of a wild-type control strain. Both strains
284 harbor molecular barcodes to distinguish between the two strains using oligonucleotide
285 probes complementary to each barcode allele. In short, ten L4 individuals of each strain
286 were placed onto a single 6 cm NGMA plate along with ten L4 individuals of the PTM229
287 strain (an N2 strain that contains a synonymous change in the *dpy-10* locus that does not
288 have any growth effects compared to the normal laboratory N2 strain (Zhao et al., 2018)).
289 Ten independent NGMA plates of each competition were prepared for each strain in each
290 test condition, control (DMSO) or BZ (albendazole and DMSO). We prepared ten
291 replicates of each competition, except the deletion allele of *ben-1*, which only had six
292 replicates of the control condition because of contamination on four of the plates. The N2,

293 F200Y (*ean101*), and *ben-1* deletion (*ean64*) strains were included to ensure that assays
294 were reproducible and that all plates had an effective albendazole concentration (Hahnel
295 et al., 2018). Plates were grown for roughly one week to starvation. Animals were
296 transferred to a new plate of the same condition by transferring a 0.5 cm³ NGMA piece
297 from the starved plate onto the new plate. The remaining individuals on the starved plate
298 were washed into a 15 mL Falcon tube with M9 buffer, concentrated by allowing the
299 animals to settle for roughly one hour, and stored at -80°C. DNA was extracted using the
300 DNeasy Blood & Tissue kit (Qiagen 69506). Competitions were performed for seven
301 generations, and animals were collected after generations, one, three, five, and seven.

302 We quantified the relative allele frequency of each strain as previously described
303 (Zhao et al., 2018). In short, a digital PCR approach with TaqMan probes (Applied
304 Biosciences) was used. Extracted genomic DNA was digested with *EcoRI* for 30 minutes
305 at 30°C, purified with Zymo DNA cleanup kit (D4064), and diluted to approximately 1
306 ng/μL. Using TaqMan probes as described previously (Zhao et al., 2018), the digital PCR
307 assay was performed with a Bio-Rad QX200 device with standard probe absolute
308 quantification settings. The TaqMan probes bind to wild-type *dpy-10* and the *dpy-10* allele
309 present in PTM229 selectively. Relative allele frequencies of each tested allele were
310 calculated using the QuantaSoft software and default settings. Calculations of relative
311 fitness were calculated by linear regression analysis to fit the data to a one-locus generic
312 selection model (Zhao et al., 2018).

313

314 **2.6 Statistical analyses**

315 All statistical comparisons were performed in *R* version 3.6.1 (Core Team and
316 Others, 2013) with the *Rstatix* package. The *tukeyHSD* function was used on an ANOVA
317 model with the formula *phenotype* ~ *strain* to calculate differences between population trait

318 values. The EC50 values for the fenbendazole dose response assay were calculated
319 using the *drc* function from the *drc* package with `fct = LL.3` (Ritz et al., 2015).

320

321 **2.7 Research Data**

322 S1 contains dose-response curve data for albendazole treatment. S2 contains
323 regressed data at high-replication for albendazole treatment for canonical alleles. S3
324 contains regressed data at high-replication for albendazole treatment for newly identified
325 alleles. S4 contains dose-response curve data for fenbendazole treatment. S5 contains
326 regressed data at high-replication for fenbendazole treatment for canonical alleles. S6
327 contains regressed data at high-replication for albendazole treatment for newly identified
328 alleles. S7 contains regressed data at high-replication for fenbendazole treatment for all
329 alleles. S8 contains raw phenotype data for DMSO conditions. S9 contains calculated
330 EC50 values for each allele. S10 contains the calculated allele frequency for the
331 competitive fitness assay in albendazole and DMSO. S11 contains calculated competitive
332 fitness values in albendazole and DMSO. S12 contains allele designation to ECA
333 translations. S13 is an xlsx file with raw ddPCR data from the competitive fitness assay.
334 Supplemental Table 1 contains a list of all strains along with genotypes and strain
335 designations. Supplemental Table 2 contains all oligonucleotides used in the study for
336 CRISPR, PCR, and allele frequency calculations. All tables, datasets, along with code for
337 analysis and generation of figures can be found at GitHub
338 (https://github.com/AndersenLab/ben1_2020_CMD).

339

340

341

342

343

344

345

346

347

348

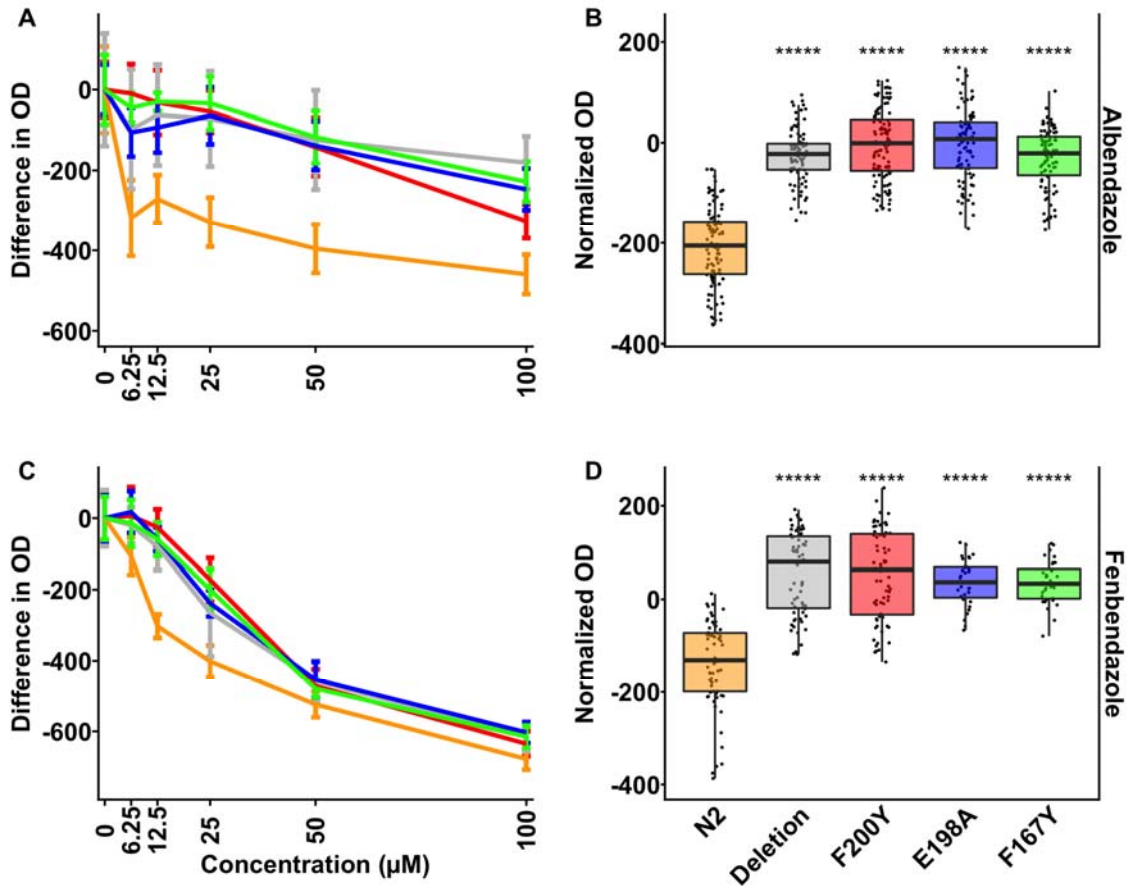
349 **3. Results**

350

351 **3.1 All three canonical parasitic nematode beta-tubulin alleles confer BZ resistance**

352 We performed BZ dose-response assays on strains with the three canonical
353 parasitic nematode beta-tubulin alleles (F200Y, F167Y, and E198A) along with positive
354 and negative controls for albendazole effects (N2 and the *ben-1* deletion allele,
355 respectively). All strains were generated in the N2 background, so the allele at the *ben-1*
356 locus is the only difference between the genome-edited strain and the unedited parent
357 strain. The BZ response assays used a flow-based device to measure the optical densities
358 of hundreds of animals in each of 12 replicate cultures per strain (see Methods). Optical
359 density refers to the amount of the laser light that is obstructed by an individual integrated
360 over the amount of time that the individual interrupts the laser. Optical density was used to
361 quantify BZ responses as a proxy for nematode health because *C. elegans* grows longer
362 and more dense as it develops. A decrease in optical density represents a developmental
363 delay, which is commonly observed in responses to BZ treatments (Driscoll et al., 1989;
364 Hahnel et al., 2018; Zamanian et al., 2018). This experimental setup allowed us to
365 determine whether the parasitic nematode beta-tubulin alleles quantitatively caused
366 resistance as compared to the sensitive wild-type *ben-1* allele and the resistant *ben-1*
367 deletion allele (**Fig. 1**). We tested the BZ responses of these strains to either albendazole
368 or fenbendazole. We also tested for developmental defects in control conditions, which
369 would indicate detrimental fitness effects, but did not detect any defects. Surprisingly, the

370 F167Y strain developed faster than the wild-type strain in control conditions
371 (Supplemental Fig. 2).
372



373

374 **Fig. 1. Quantitative responses of canonical parasite beta-tubulin alleles to**
375 **albendazole and fenbendazole**

376 Drug-response assays for three canonical parasite beta-tubulin alleles, F200Y, E198A,
377 and F167Y, are shown. (A, C) Normalized values were calculated by subtracting the mean
378 optical density in a strain from each population measurement. Normalized trait values are
379 shown in response to six drug concentrations (0, 6.25, 12.5, 25, 50, and 100 μM) of BZ.
380 (B, D) Regressed optical density values of responses to 30 μM BZ at high-replication are
381 shown on the y-axis. Each point represents a regressed optical density value calculated
382 per well containing approximately 35-50 animals. Significant differences between N2 and
383 all other strains are shown as asterisks above the data from each strain (p < 0.001 = ***, p

384 <0.0001 = ****, Tukey HSD). (A) and (B) show responses to albendazole; (C) and (D)
385 show responses to fenbendazole.

386

387 Albendazole and fenbendazole caused different phenotypic effects on the set of *C.*
388 *elegans* strains. In response to albendazole (**Fig. 1A,B**), the wild-type laboratory strain
389 was sensitive, measured as a large decrease in development rate (decreased animal
390 optical density) even at the lowest concentration of albendazole. As concentrations
391 increased, the laboratory strain was only marginally more affected. By contrast, the *ben-1*
392 deletion strain was resistant at all concentrations, including the highest concentrations of
393 albendazole. The three canonical parasitic nematode beta-tubulin alleles had dose-
394 response curves statistically similar to the *ben-1* deletion strain, which suggests they
395 conferred equal levels of resistance. To determine subtle albendazole effects among the
396 strains, we measured development in the presence of 30 μ M albendazole for each strain
397 at high replication. The three canonical parasitic nematode beta-tubulin strains were
398 statistically indistinguishable from the *ben-1* deletion strain and were significantly more
399 resistant than the wild-type strain (**Fig. 1B**).

400 Fenbendazole caused more drastic changes to *C. elegans* development in a dose-
401 dependent manner (**Fig. 1C,D**). The wild-type laboratory strain showed significant
402 developmental delays across the range of doses studied. Unlike albendazole, each of the
403 *ben-1* mutant alleles (including the *ben-1* loss-of-function deletion allele) also showed
404 developmental defects as the concentration of fenbendazole increased. At the 100 μ M
405 fenbendazole dose, all of the strains were severely developmentally delayed. To
406 determine subtle fenbendazole effects among the strains, we measured growth in the
407 presence of 30 μ M fenbendazole for each strain at high replication. Again, the three
408 canonical parasitic nematode beta-tubulin strains responded similarly to the *ben-1* deletion
409 strain and were less sensitive to fenbendazole as compared to the wild-type control strain

410 **(Fig. 1D)**. For each genome-edited allele, we tested two independently generated strains,
411 and all independent strain duplicates showed similar responses across all doses of both
412 BZ compounds and at high-replication **(Supplemental Fig. 3, Supplemental Fig. 4)**.

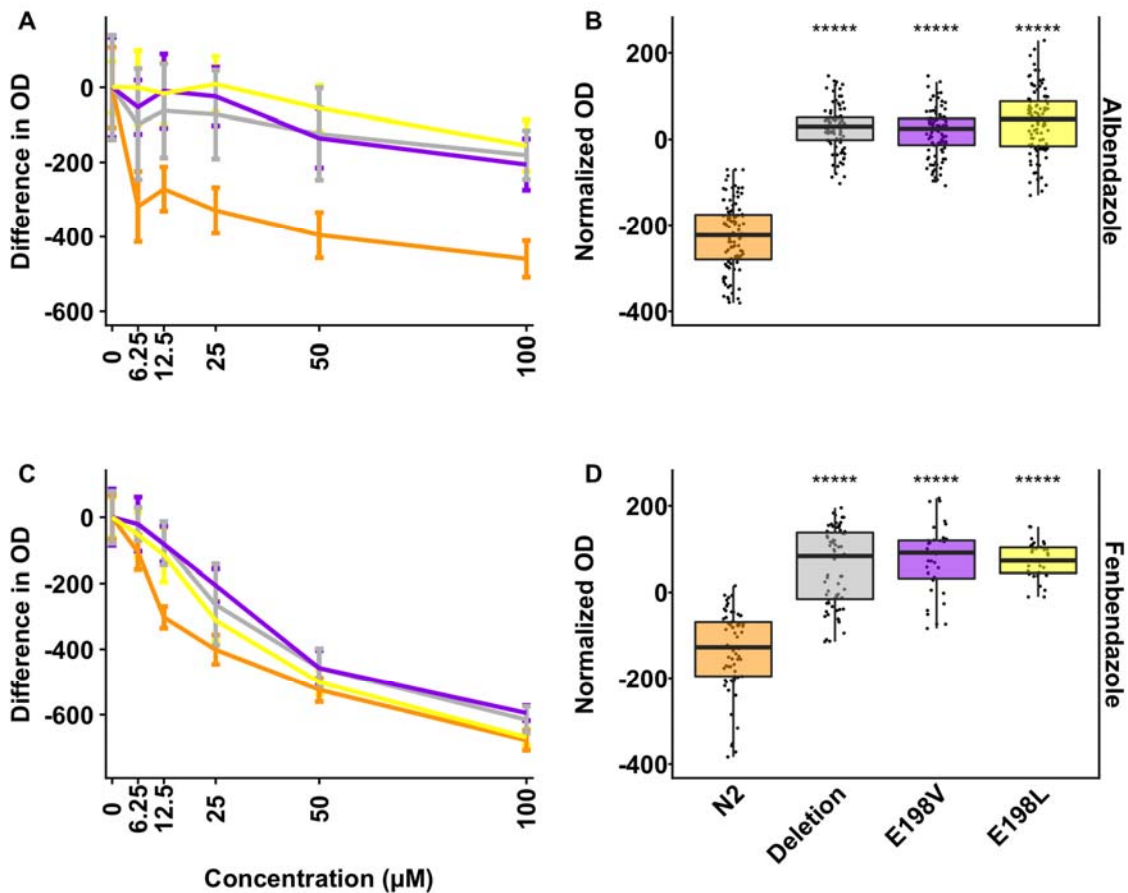
413 The results of the dose-response and the high-replication assays indicated that the
414 canonical parasitic nematode beta-tubulin alleles conferred resistance to BZs **(Fig. 1,**
415 **Supplemental Fig. 5)**. The wild-type strain had a lower EC50 than any of the canonical
416 parasitic nematode beta-tubulin alleles, because it is more sensitive to BZ treatment. The
417 EC50 values for the canonical parasitic nematode beta-tubulin alleles were statistically the
418 same, which suggested that these alleles conferred the same quantitative level of
419 resistance. We could not calculate EC50 values in albendazole because the full range of
420 phenotypic responses required higher concentrations than tested. Regardless, the change
421 in responses among the canonical parasitic nematode beta-tubulin alleles and the
422 susceptible wild-type strain was apparent. These results demonstrated that each of the
423 three canonical parasitic nematode beta-tubulin alleles caused resistance to albendazole
424 and fenbendazole.

425

426 **3.2 Two of the less frequently observed parasitic nematode beta-tubulin alleles also** 427 **confer BZ resistance**

428 Other beta-tubulin alleles beyond the canonical alleles have been identified using
429 population sequencing approaches (Avramenko et al., 2019; Mohammedsalih et al., 2020;
430 Redman et al., 2015). These alleles are not present in all parasites in a population, so they
431 might confer different levels of BZ resistance and/or effects on growth. We introduced the
432 E198V and E198L alleles into the N2 genetic background to perform quantitative drug
433 response assays using the same flow-based measurement and experimental design as
434 previously described. In response to albendazole, both the E198V and E198L strains
435 responded similarly to the *ben-1* deletion strain at each BZ concentration **(Fig. 2A)**. Next,

436 we performed a high-replication experiment to determine if the edited beta-tubulin alleles
437 conferred small differences in albendazole resistance at 30 μ M. As previously observed
438 with the canonical parasitic nematode beta-tubulin alleles, both E198V and E198L showed
439 statistically the same response to albendazole as the *ben-1* deletion strain (**Fig. 2B**). In
440 fenbendazole, the results followed the same pattern as observed in the canonical parasitic
441 nematode beta-tubulin alleles (**Fig. 2C,D**). Except for the highest fenbendazole
442 concentrations, both E198V and E198L were developmentally delayed but to a lesser
443 extent than the susceptible N2 strain (**Fig. 2C**). At 50 μ M fenbendazole, N2 and the
444 mutant *ben-1* strains were statistically indistinguishable from each other and all showed
445 significant developmental delays. At high-replication, E198V and E198L were statistically
446 more resistant than N2 ($p < 0.0001$, Tukey HSD) but not different from the *ben-1* deletion
447 strain at 30 μ M fenbendazole (**Fig. 2D**). All of the tested beta-tubulin alleles conferred the
448 same fenbendazole response as shown by the EC50 estimates (**Supplemental Fig. 5**).
449 Similar to what we found with the canonical parasitic nematode beta-tubulin alleles, the
450 two independently generated genome-edited strains for each of the E198V and E198L
451 alleles were not significantly different from each other in the dose-response assay
452 (**Supplemental Fig. 3**) or the high-replication single-dose assay (**Supplemental Fig. 4**).
453 Additionally, E198V and E198L were tested in control conditions and showed no
454 significant differences from the N2 strain, which suggested that they do not cause viability
455 defects in this single-generation assay (**Supplemental Fig. 2**).



456

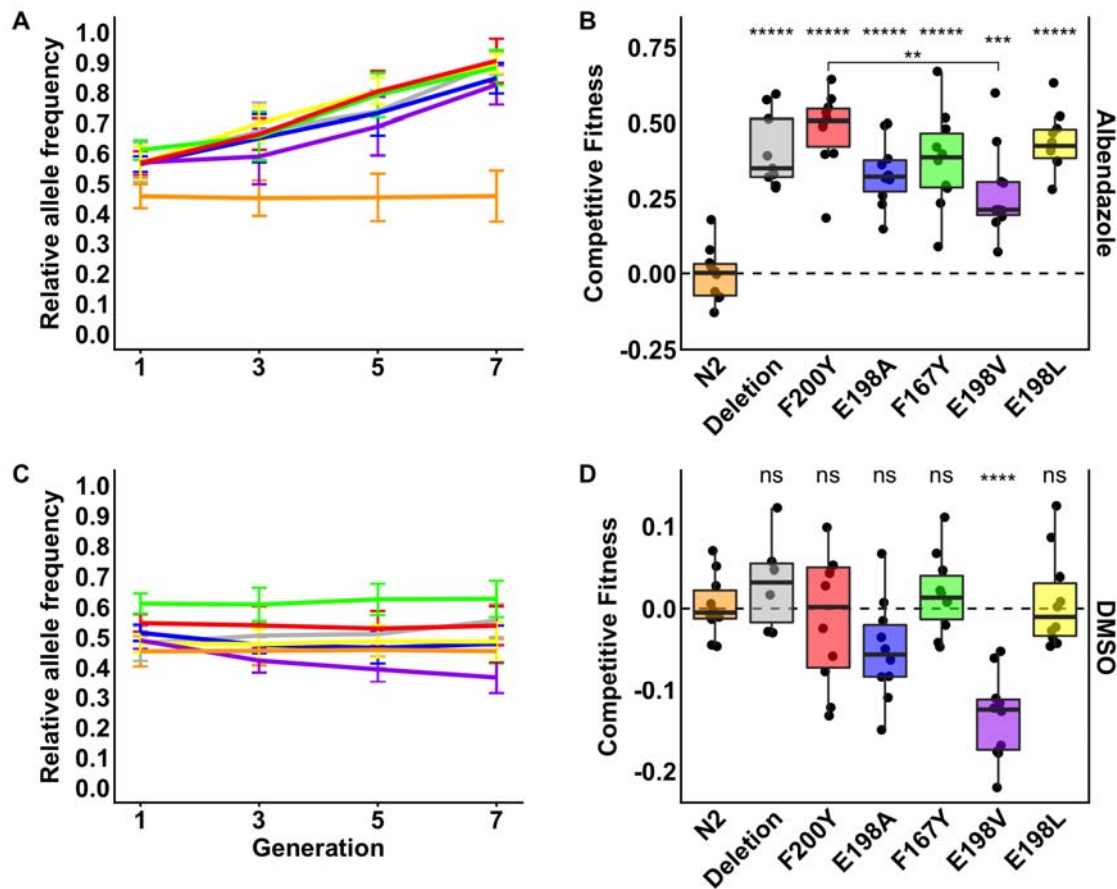
457 **Fig. 2. Quantitative responses to albendazole and fenbendazole conferred by the**
458 **E198V and E198L alleles**

459 Drug-response assays for two of the non-canonical parasitic nematode beta-tubulin
460 alleles, E198V and E198L, are shown. (A, C) Normalized values were calculated by
461 subtracting the mean trait value measured for a population of individuals in the control
462 condition (0 μM BZ) from the trait values measured for a population of individuals at all BZ
463 concentrations (0, 6.25, 12.5, 25, 50, and 100 μM). (B, D) Regressed optical density
464 values of responses to 30 μM BZ at high-replication are shown on the y-axis. Each point
465 represents a regressed optical density value calculated per well containing approximately
466 35-50 animals. Significant differences between N2 and all other strains are shown as
467 asterisks above the data from each strain ($p < 0.001 = ***, p < 0.0001 = ****$, Tukey HSD).
468 (A) and (B) show responses to albendazole; (C) and (D) show responses to fenbendazole.

469

470 **3.3 Multi-generational competitive fitness assays quantify albendazole selection**
471 **and growth effects caused by beta-tubulin alleles**

472



473

474 **Fig. 3. Variation in competitive fitness among *ben-1* alleles in both albendazole and**
475 **control conditions**

476 (A) Results from a multi-generational competition assay between a barcoded N2 strain
477 and a strain of each edited beta-tubulin strain in albendazole conditions. Generation
478 number is shown on the x-axis, and relative allele frequencies are plotted on the y-axis.

479 (B) Tukey box plots of log₂-transformed competitive fitness values in albendazole
480 conditions are shown. The tested allele is shown on the x-axis, and competitive fitness
481 values as compared to the wild-type strain are plotted on the y-axis. Each point represents
482 the competitive fitness of a biological replicate. Significant differences between N2 and all
483 other strains are shown as asterisks above the data from each strain (p < 0.001 = ***, p

484 <0.0001 = ****, Tukey HSD). The level of significance between the F200Y and E198V
485 strains is shown as a bracket ($p < 0.01$, Tukey HSD). (C) Results from multi-generational
486 pairwise competition assays in DMSO control conditions are plotted as in (A). (D) Tukey
487 box plots of competitive fitness in control DMSO conditions are shown as in (B).
488 Significant differences between N2 and all other strains are shown as asterisks above the
489 data from each strain ($p < 0.0001 = ****$, Tukey HSD).

490

491 We performed multi-generational assays to measure competitive fitness effects
492 between strains with the parasitic nematode beta-tubulin alleles and the wild-type *ben-1*
493 allele. This assay is more sensitive than our previous single-generation high-throughput
494 assays because differences in reproductive rate also influence fitness. Additionally, small
495 changes in fitness are more easily observed as they accumulate over multiple
496 generations. If an allele confers a deleterious fitness effect compared to the wild-type
497 strain, then that strain will decrease in frequency over the generations of the competition
498 assay. Conversely, if an allele confers a beneficial effect compared to the wild-type allele,
499 then that strain will increase in frequency over the generations of the competition assay.
500 Finally, if an allele has no difference in effect compared to the wild-type allele, then the two
501 strains would be found at approximately equal frequencies over the generations of the
502 competition assay. The N2, *ben-1* deletion, and the F200Y strains have been tested in
503 both albendazole and control conditions previously (Hahnel et al., 2018). The wild-type
504 strain showed no differences in competitive fitness in either control or albendazole
505 conditions compared to the barcoded wild-type control strain (**Fig 3**). As demonstrated
506 previously (Hahnel et al., 2018), the F200Y and the *ben-1* deletion strains had no fitness
507 consequences in control conditions but had growth advantages in BZ conditions. In
508 albendazole conditions, we expected that all parasite beta-tubulin alleles would confer
509 resistance in multi-generational assays because we observed resistance in the high-

510 throughput assays (**Fig. 1, Fig. 2**). Therefore, the frequencies of the parasite beta-tubulin
511 alleles should increase over time in albendazole conditions. As expected, all edited alleles
512 showed a steady increase in frequency (as compared to the wild-type strain) across each
513 subsequent generation in albendazole conditions (**Fig. 3A**). The allele frequencies as
514 compared to the wild-type control strain can be used to calculate competitive fitness. We
515 found that each edited allele conferred significant competitive advantages in albendazole
516 conditions (**Fig. 3B**). However, the E198V allele was significantly more developmentally
517 delayed than the F200Y allele across the seven generations of albendazole selection ($p <$
518 0.01 , Tukey HSD) (**Fig. 3A,B**).

519 Because the multi-generational assays might be more sensitive than the high-
520 throughput assays, we wanted to compete strains in control conditions to investigate
521 whether any parasite beta-tubulin alleles confer fitness disadvantages without the
522 presence of drug selection. We found no deleterious effects in the high-throughput assays,
523 so we expected that all alleles would be equally fit in the multi-generational assays. In
524 control conditions, only the E198V allele conferred a difference in growth, decreasing in
525 abundance compared to the wild-type strain over seven generations (**Fig. 3C**). Based on
526 the competitive fitness values, this strain was significantly less fit than the wild-type strain
527 in control growth conditions ($p < 0.0001$, Tukey HSD) (**Fig. 3D**). This decrease suggests
528 that strains with the E198V allele can be outcompeted in normal conditions by strains with
529 the wild-type allele at the *ben-1* locus.

530

531

532

533

534

535

536

537 **4. Discussion**

538 **4.1 Parasitic nematode beta-tubulin alleles confer BZ resistance**

539 After exposure to BZ compounds, the frequencies of certain beta-tubulin alleles
540 increase in parasitic nematode populations, including F167Y, E198A, E198I, E198K,
541 E198L, E198V, E198Stop, and F200Y (Avramenko et al., 2019; Ghisi et al., 2007; Kwa et
542 al., 1994; Mohammedsalih et al., 2020; Redman et al., 2015; von Samson-Himmelstjerna
543 et al., 2009; Silvestre and Cabaret, 2002). These alleles have long been hypothesized to
544 cause BZ resistance, but the lack of controlled genetic backgrounds and genome-editing
545 tools have made it difficult to test this hypothesis in parasitic nematode species. Previous
546 studies have used *C. elegans* overexpression experiments to show that beta-tubulin is
547 sufficient to restore BZ susceptibility (Kwa et al., 1995). Since the introduction of the
548 CRISPR-Cas9 system in *C. elegans*, experiments on gene function at the single amino
549 acid level have become possible. We used genome editing to independently introduce five
550 parasitic nematode beta-tubulin alleles, F167Y, E198A, E198L, E198V, and F200Y, into
551 the *C. elegans ben-1* locus in a defined genetic background. We tested each of these
552 alleles using both high-replication growth assays and competitive fitness assays in BZ and
553 control conditions. We found all alleles conferred the same level of resistance to
554 albendazole and fenbendazole in the high-replication growth assays that encompass a
555 single generation. However, we found in multi-generational competitive fitness assays that
556 the E198V allele confers lower resistance in albendazole conditions than the F200Y allele.
557 Additionally, the E198V allele also had decreased fitness compared to the wild-type strain
558 in control conditions. Our results definitively prove that these beta-tubulin alleles confer BZ
559 resistance and that some of these alleles can also affect fitness in laboratory conditions.

560 The two assays used in this study have different advantages and disadvantages.
561 The high-replication high-throughput assay provides an excellent platform for quickly

562 quantifying if an allele confers resistance to BZs. The assay enables high levels of
563 replication. One disadvantage of this assay is that traits are measured after only one
564 generation of growth under drug selection, which could fail to identify subtle differences in
565 fitness or resistance. By contrast, the multigenerational competition assay enables the
566 measurement of small differences between the edited alleles and the wild-type strain over
567 seven generations, which can detect subtle differences in fitness or resistance. Each
568 generation compounds the fitness impacts of the edited alleles. These assays in
569 combination provide a powerful platform to determine levels of resistance and potential
570 fitness consequences.

571 Our ability to test beta-tubulin benzimidazole resistance alleles in a high-throughput
572 and sensitive manner enables the study of additional alleles. In this study, we tested five
573 of the eight alleles identified in parasite populations. The E198I, E198K, and E198Stop
574 alleles still need to be tested in defined genetic backgrounds. In addition to testing if these
575 alleles confer resistance, we can use the multigenerational competition assays to assess
576 whether they confer any fitness effects. The results of these experiments can be used to
577 implement proper management of resistance to benzimidazoles in field populations. For
578 example, knowledge about quantitative levels of BZ resistance can alter anthelmintic
579 treatment strategies if high BZ resistance alleles are detected in populations. Importantly,
580 the field requires cheap, point-of-care diagnostic tests for validated resistance alleles. If
581 we had a complete catalog of resistance alleles, veterinarians and farmers could more
582 easily maintain refugia populations and control benzimidazole resistance.

583

584 **4.2 Differential responses to albendazole and fenbendazole in *C. elegans***

585 Albendazole and fenbendazole are both widely used anthelmintic compounds that
586 often treat similar parasitic nematode species. However, these compounds have different
587 levels of effectiveness and safety on host species. For example, albendazole has

588 previously been shown to have teratogenic effects in pregnant rats and sheep (Capece et
589 al., 2003; Navarro et al., 1998). By contrast, the primary fenbendazole metabolite in
590 ruminants, oxibendazole, showed no toxic effects on pregnant mice, rats, sheep, or cattle
591 (Theodorides et al., 1977). In addition to differential responses in the host species treated
592 with albendazole or fenbendazole, parasitic nematodes respond differently to these two
593 compounds. A recent study found that, in response to albendazole, fewer genes are
594 differentially expressed compared to fenbendazole (Stasiuk et al., 2019). Our study also
595 found differential responses to albendazole and fenbendazole, where *C. elegans* was
596 overall less susceptible to albendazole than fenbendazole. Only the highest albendazole
597 concentrations caused detrimental effects on the strains with parasitic nematode beta-
598 tubulin alleles. By contrast, fenbendazole caused detrimental effects on all strains at all
599 concentrations. The difference in these responses suggests that future studies of beta-
600 tubulin copy number, tissue-specificity, and specific drug interactions could be fruitful.

601 One possibility underlying this difference in response is that fenbendazole might
602 have additional targets beyond beta-tubulin, including genes that encode beta-tubulin
603 interacting proteins. Additionally, the *C. elegans* laboratory wild-type strain N2 has five
604 beta-tubulin genes beyond *ben-1*, which could provide targets for fenbendazole. The two
605 most highly expressed beta-tubulins, *tbb-1* and *tbb-2*, harbor the resistant tyrosine at the
606 200 position making them less than ideal candidates. However, it is possible that
607 fenbendazole binds these beta-tubulins with lower affinity. Previous studies have
608 discovered additional loci that underlie differential responses to fenbendazole (Zamanian
609 et al., 2018), and the loci are not shared between albendazole and fenbendazole. These
610 loci could be BZ compound specific. Moreover, studies of gene expression in response to
611 different BZ compounds have shown that fenbendazole exposure causes more
612 differentially expressed genes than albendazole (Stasiuk et al., 2019). Many of these
613 genes encode enzymes essential for biotransformation, including cytochrome P450 family

614 members, nuclear hormone receptors, and UDP-glucuronosyltransferases. To make more
615 BZ compounds effective across more parasitic nematode species, we must better
616 understand these BZ-specific effects.

617

618 **4.3 Benzimidazole resistance supersedes detrimental fitness costs caused by beta-** 619 **tubulin alleles**

620 In the field, parasitic nematodes must balance responses to abiotic stresses, like
621 anthelmintic drugs, and growth. For example, alleles that confer extremely high levels of
622 resistance, but also cause severe detrimental fitness consequences, will be strongly
623 selected when BZs are used on the population. However, these same alleles will quickly
624 be selected against when the drug is removed. The selective pressure caused by the
625 anthelmintic drug must be greater than the reduced fitness caused by the resistance allele
626 when the drug is removed. Alleles that confer resistance and have no fitness
627 consequences will be maintained in field populations. This argument could be one reason
628 why we only find specific beta-tubulin alleles across parasite populations.

629 The multi-generational competitive fitness assays can be used to investigate this
630 balance by comparing relative fitness in drug and control conditions. We found that all
631 parasitic nematode beta-tubulin alleles conferred resistance to albendazole over seven
632 generations when competed against wild-type animals (**Fig. 3**). However, some alleles
633 caused different levels of resistance to albendazole. The E198V allele conferred
634 significantly lower levels of albendazole resistance than the F200Y allele, and the E198V
635 allele was also the only allele to confer detrimental fitness in control conditions. This
636 results suggests that this allele could be less advantageous than other beta-tubulin alleles
637 in that it causes less BZ resistance and decreased fitness. Matching these results, this
638 allele is found at low frequencies in field populations (Avramenko et al., 2019). The E198V
639 allele might be selected when BZ drugs are used, but when the drug is removed from a

640 population, this allele would cause a fitness detriment and not be maintained in the
641 population. Conversely, all of the other tested alleles showed no detrimental fitness
642 consequences when the drug is not present. These results suggest that, in field
643 populations with persistent BZ resistance after removal of treatment (van Wyk et al.,
644 1997), the beta-tubulin allele might also persist because of the lack of fitness cost.

645 Our results can be explained by this balance between BZ resistance and fitness
646 costs, but it is still not clear why parasite populations harbor low frequency E198V alleles
647 and higher frequencies of the E198L allele (Avramenko et al., 2019; Mohammedsalih et
648 al., 2020). The E198L allele can only be generated after changing two nucleotides, and
649 the E198V allele is one of those changes (**Supplemental Figure 1**). Why would a parasite
650 population make the two-step transition from wild-type to E198V to E198L, instead of a
651 single step to one of the canonical alleles, like E198A? As we showed, the E198A allele is
652 equally resistant to albendazole as E198L and neither alleles seems to confer a fitness
653 cost (**Fig 3**). One explanation is that some or all beta-tubulin alleles confer dominant
654 resistance to BZ compounds. It is not known the allelic status in field populations, and we
655 only tested homozygous *C. elegans* strains in our assays. Heterozygous animals
656 harboring the E198V allele might be resistant to BZ compounds, and other alleles might
657 only be resistant when homozygous. In that way, resistance conferred in heterozygous
658 individuals can be selected for additional changes that will change the E198V allele to an
659 allele that does not cause a fitness cost. Dominance relationships for these alleles must
660 be tested in characterized genetic backgrounds and sensitive BZ assays. Resistance
661 conferred by each allele in a heterozygote could also vary, and the ordering of the
662 resistance in heterozygotes could help us understand the speed at which resistance can
663 spread through a population. Another explanation for this disparity in the frequencies of
664 alleles across resistant populations could be the codon preference in the target species.
665 Previous work found that codon preference can vary dramatically among species (Mitreva

666 et al., 2006). If the codon preference of a species favors a transition to E198V instead of
667 E198A that could help explain this transition. Another explanation could be suggested by a
668 non-significant trend observed in our competitive fitness assay where we found that the
669 E198A allele appeared to confer a fitness detriment as compared to F167Y, E198L, and
670 F200Y in albendazole (**Fig 3A,B**). The E198A allele appears to more closely resemble the
671 E198V allele in competitive fitness over seven generations than the other tested alleles.
672 However, we require increased levels of replication to identify if this trend is significant.

673 The balance between BZ resistance and fitness costs are also influenced by the
674 complement of beta-tubulin genes present in a species and the tissues and times in which
675 they are expressed. For example, *C. elegans* has six beta-tubulin genes and some of
676 these have been shown to be at least partially functionally redundant with each other (Ellis
677 et al., 2004). Importantly, the two most highly expressed beta-tubulin genes are *tbb-1* and
678 *tbb-2*, and both of these genes encode beta-tubulins that should be resistant to BZ
679 treatments. *H. contortus* only has four beta-tubulin genes and the two most highly
680 expressed are sensitive to BZ treatments (Saunders et al., 2013). This lack of redundancy
681 and prevalent drug sensitivity could explain both the kinetics of resistance and the
682 persistence of alleles across populations. Competitive fitness assays would be difficult to
683 perform in *H. contortus* because of the previously discussed issues of lack of a controlled
684 genetic background and genome-editing tools. However, one possibility to get around this
685 obstacle is to make the *C. elegans* complement of beta-tubulin more like *H. contortus*.
686 Removal of redundant beta-tubulin genes in *C. elegans* would study the effects of these
687 alleles in a model closer to the situation in *H. contortus* populations. Overall, the balance
688 parasites must maintain between anthelmintic resistance and maintenance of competitive
689 fitness when drugs are not present is an extremely relevant approach to understand
690 anthelmintic effectiveness.

691

692 **4.4 Future avenues and methods of research**

693 The approach described here shows that hypotheses generated from the study of
694 parasitic nematode populations can be tested and measured using the model *C. elegans*.
695 Future studies of homozygous and heterozygous resistance could impact parasitic
696 nematode control in field populations. Additionally, the generation of more *H. contortus*-
697 like models using *C. elegans* will allow for more accurate replication of the natural
698 situations in which alleles exist. The continued interplay of research in *C. elegans* and
699 parasite species allows for quick validation of resistance alleles and measurement of any
700 fitness consequences associated with the identified alleles.

701

702 **Declaration of competing interests**

703 The authors have no competing financial or personal interests that impacted the
704 work presented in this paper.

705

706 **Acknowledgements**

707 We would like to thank Katie Evans, Robyn Tanny, Sam Widmayer, and Janneke Wit for
708 their feedback and comments on this manuscript. C.M.D. was supported by the
709 Biotechnology Training Program at Northwestern University (T32 GM008449). S.R.H. was
710 funded by a DFG fellowship (HA 8449/1-1) from the Deutsche Forschungsgemeinschaft.
711 E.C.A. was funded by the National Institutes of Health NIAID grant R21AI121836. This
712 study would not have been possible without data from Wormbase, the *Caenorhabditis*
713 Genetics Center (P40 OD010440), and the *Caenorhabditis elegans* Natural Diversity
714 Resource (NSF CSBR 1930382). The funding sources had no impact on the design of this
715 study. We would also like to thank Samantha Peters for her illustrations of *C. elegans* and
716 *H. contortus*.

717

718

719

720

721

722

723 **References**

724 Andersen, E.C., Bloom, J.S., Gerke, J.P., and Kruglyak, L. (2014). A variant in the neuropeptide
725 receptor npr-1 is a major determinant of *Caenorhabditis elegans* growth and physiology. *PLoS*
726 *Genet.* *10*, e1004156.

727 Avramenko, R.W., Redman, E.M., Melville, L., Bartley, Y., Wit, J., Queiroz, C., Bartley, D.J., and
728 Gilleard, J.S. (2019). Deep amplicon sequencing as a powerful new tool to screen for sequence
729 polymorphisms associated with anthelmintic resistance in parasitic nematode populations.
730 *International Journal for Parasitology* *49*, 13–26.

731 Boyd, W.A., Smith, M.V., and Freedman, J.H. (2012). *Caenorhabditis elegans* as a model in
732 developmental toxicology. *Methods Mol. Biol.* *889*, 15–24.

733 Brady, S.C., Zdraljevic, S., Bisaga, K.W., Tanny, R.E., Cook, D.E., Lee, D., Wang, Y., and
734 Andersen, E.C. (2019). A Novel Gene Underlies Bleomycin-Response Variation in *Caenorhabditis*
735 *elegans*. *Genetics* *212*, 1453–1468.

736 Campbell, W.C., and Cuckler, A.C. (1962). Thiabendazole treatment of the invasive phase of
737 experimental trichinosis in swine. *Ann. Trop. Med. Parasitol.* *56*, 500–505.

738 Capece, B.P.S., Navarro, M., Arcalis, T., Castells, G., Toribio, L., Perez, F., Carretero, A., Ruberte,
739 J., Arboix, M., and Cristòfol, C. (2003). Albendazole Sulphoxide Enantiomers in Pregnant Rats
740 Embryo Concentrations and Developmental Toxicity. *The Veterinary Journal* *165*, 266–275.

741 Charlier, J., Höglund, J., von Samson-Himmelstjerna, G., Dorny, P., and Vercruysse, J. (2009).

- 742 Gastrointestinal nematode infections in adult dairy cattle: Impact on production, diagnosis and
743 control. *Veterinary Parasitology* *164*, 70–79.
- 744 Core Team, R., and Others (2013). R: a language and environment for statistical computing. R
745 Foundation for Statistical Computing, Vienna.
- 746 Crook, E.K., O'Brien, D.J., Howell, S.B., Storey, B.E., Whitley, N.C., Burke, J.M., and Kaplan, R.M.
747 (2016). Prevalence of anthelmintic resistance on sheep and goat farms in the mid-Atlantic region
748 and comparison of in vivo and in vitro detection methods. *Small Rumin. Res.* *143*, 89–96.
- 749 Driscoll, M., Dean, E., Reilly, E., Bergholz, E., and Chalfie, M. (1989). Genetic and molecular
750 analysis of a *Caenorhabditis elegans* beta-tubulin that conveys benzimidazole sensitivity. *J. Cell*
751 *Biol.* *109*, 2993–3003.
- 752 Ellis, G.C., Phillips, J.B., O'Rourke, S., Lyczak, R., and Bowerman, B. (2004). Maternally
753 expressed and partially redundant β -tubulins in *Caenorhabditis elegans* are autoregulated. *J. Cell*
754 *Sci.* *117*, 457–464.
- 755 Evans, K.S., and Andersen, E.C. (2020). The Gene *scb-1* Underlies Variation in *Caenorhabditis*
756 *elegans* Chemotherapeutic Responses. *G3* .
- 757 García-González, A.P., Ritter, A.D., Shrestha, S., Andersen, E.C., Yilmaz, L.S., and Walhout,
758 A.J.M. (2017). Bacterial Metabolism Affects the *C. elegans* Response to Cancer
759 Chemotherapeutics. *Cell* *169*, 431–441.e8.
- 760 Ghisi, M., Kaminsky, R., and Mäser, P. (2007). Phenotyping and genotyping of *Haemonchus*
761 *contortus* isolates reveals a new putative candidate mutation for benzimidazole resistance in
762 nematodes. *Vet. Parasitol.* *144*, 313–320.
- 763 Hahnel, S.R., Zdraljevic, S., Rodriguez, B.C., Zhao, Y., McGrath, P.T., and Andersen, E.C. (2018).
764 Extreme allelic heterogeneity at a *Caenorhabditis elegans* beta-tubulin locus explains natural
765 resistance to benzimidazoles. *PLoS Pathog.* *14*, e1007226.
- 766 Hastie, A.C., and Georgopoulos, S.G. (1971). Mutational resistance to fungitoxic benzimidazole

- 767 derivatives in *Aspergillus nidulans*. *J. Gen. Microbiol.* *67*, 371–373.
- 768 Hinney, B., Schoiswohl, J., Melville, L., Ameen, V.J., Wille-Piazzai, W., Bauer, K., Joachim, A.,
769 Krücken, J., Skuce, P.J., and Krametter-Frötscher, R. (2020). High frequency of benzimidazole
770 resistance alleles in trichostrongyloids from Austrian sheep flocks in an alpine transhumance
771 management system. *BMC Vet. Res.* *16*, 132.
- 772 Hodgkinson, J.E., Kaplan, R.M., Kenyon, F., Morgan, E.R., Park, A.W., Paterson, S., Babayan,
773 S.A., Beesley, N.J., Britton, C., Chaudhry, U., et al. (2019). Refugia and anthelmintic resistance:
774 Concepts and challenges. *International Journal for Parasitology: Drugs and Drug Resistance* *10*,
775 51–57.
- 776 Hotez, P.J., Alvarado, M., Basáñez, M.-G., Bolliger, I., Bourne, R., Boussinesq, M., Brooker, S.J.,
777 Brown, A.S., Buckle, G., Budke, C.M., et al. (2014). The global burden of disease study 2010:
778 interpretation and implications for the neglected tropical diseases. *PLoS Negl. Trop. Dis.* *8*, e2865.
- 779 Howell, S.B., Burke, J.M., Miller, J.E., Terrill, T.H., Valencia, E., Williams, M.J., Williamson, L.H.,
780 Zajac, A.M., and Kaplan, R.M. (2008). Prevalence of anthelmintic resistance on sheep and goat
781 farms in the southeastern United States. *Journal of the American Veterinary Medical Association*
782 *233*, 1913–1919.
- 783 Kahn, L.P., and Woodgate, R.G. (2012). Integrated parasite management: products for adoption by
784 the Australian sheep industry. *Vet. Parasitol.* *186*, 58–64.
- 785 Kaplan, R.M., and Vidyashankar, A.N. (2012). An inconvenient truth: global worming and
786 anthelmintic resistance. *Vet. Parasitol.* *186*, 70–78.
- 787 Kim, H., Ishidate, T., Ghanta, K.S., Seth, M., Conte, D., Jr, Shirayama, M., and Mello, C.C. (2014).
788 A co-CRISPR strategy for efficient genome editing in *Caenorhabditis elegans*. *Genetics* *197*,
789 1069–1080.
- 790 Kitchen, S., Ratnappan, R., Han, S., Leasure, C., Grill, E., Iqbal, Z., Granger, O., O’Halloran, D.M.,
791 and Hawdon, J.M. (2019). Isolation and characterization of a naturally occurring multidrug-resistant

- 792 strain of the canine hookworm, *Ancylostoma caninum*. *Int. J. Parasitol.* *49*, 397–406.
- 793 Kwa, M.S., Kooyman, F.N., Boersema, J.H., and Roos, M.H. (1993). Effect of selection for
794 benzimidazole resistance in *Haemonchus contortus* on beta-tubulin isotype 1 and isotype 2 genes.
795 *Biochem. Biophys. Res. Commun.* *191*, 413–419.
- 796 Kwa, M.S.G., Veenstra, J.G., and Roos, M.H. (1994). Benzimidazole resistance in *Haemonchus*
797 *contortus* is correlated with a conserved mutation at amino acid 200 in β -tubulin isotype 1. *Mol.*
798 *Biochem. Parasitol.* *63*, 299–303.
- 799 Kwa, M.S.G., Veenstra, J.G., Van Dijk, M., and Roos, M.H. (1995). β -Tubulin Genes from the
800 Parasitic Nematode *Haemonchus contortus* Modulate Drug Resistance in *Caenorhabditis elegans*. *J.*
801 *Mol. Biol.* *246*, 500–510.
- 802 Lustigman, S., Prichard, R.K., Gazzinelli, A., Grant, W.N., Boatman, B.A., McCarthy, J.S., and
803 Basáñez, M.-G. (2012). A research agenda for helminth diseases of humans: the problem of
804 helminthiasis. *PLoS Negl. Trop. Dis.* *6*, e1582.
- 805 Merck, and Sharp & Dohme Research Laboratories. *Animal Science Research* (1962).
806 Proceedings of a seminar on parasitic diseases with special reference to thiabendazole: Presented
807 at [the] IV Pan American Congress of Veterinary Medicine and Zootechnics, Mexico City, Nov. 13,
808 1962 (Merck Sharp & Dohme Research Laboratories).
- 809 Mitreva, M., Wendl, M.C., Martin, J., Wylie, T., Yin, Y., Larson, A., Parkinson, J., Waterston, R.H.,
810 and McCarter, J.P. (2006). Codon usage patterns in Nematoda: analysis based on over 25 million
811 codons in thirty-two species. *Genome Biol.* *7*, R75.
- 812 Mohammedsalih, K.M., Krücken, J., Khalafalla, A., Bashar, A., Juma, F.-R., Abakar, A.,
813 Abdalmalaik, A.A.H., Coles, G., and von Samson-Himmelstjerna, G. (2020). New codon 198 β -
814 tubulin polymorphisms in highly benzimidazole resistant *Haemonchus contortus* from goats in three
815 different states in Sudan. *Parasit. Vectors* *13*, 114.
- 816 Muchiut, S.M., Fernández, A.S., Steffan, P.E., Riva, E., and Fiel, C.A. (2018). Anthelmintic

- 817 resistance: Management of parasite refugia for *Haemonchus contortus* through the replacement of
818 resistant with susceptible populations. *Vet. Parasitol.* 254, 43–48.
- 819 Navarro, M., Cristofol, C., Carretero, A., Arboix, M., and Ruberte, J. (1998). Anthelmintic induced
820 congenital malformations in sheep embryos using netobimin. *Vet. Rec.* 142, 86–90.
- 821 Redman, E., Whitelaw, F., Tait, A., Burgess, C., Bartley, Y., Skuce, P.J., Jackson, F., and Gilleard,
822 J.S. (2015). The Emergence of Resistance to the Benzimidazole Anthelmintics in Parasitic
823 Nematodes of Livestock Is Characterised by Multiple Independent Hard and Soft Selective
824 Sweeps. *PLOS Neglected Tropical Diseases* 9, e0003494.
- 825 Ritz, C., Baty, F., Streibig, J.C., and Gerhard, D. (2015). Dose-Response Analysis Using R. *PLoS*
826 *One* 10, e0146021.
- 827 Roos, M.H., Boersema, J.H., Borgsteede, F.H., Cornelissen, J., Taylor, M., and Ruitenber, E.J.
828 (1990). Molecular analysis of selection for benzimidazole resistance in the sheep parasite
829 *Haemonchus contortus*. *Mol. Biochem. Parasitol.* 43, 77–88.
- 830 von Samson-Himmelstjerna, G., Walsh, T.K., Donnan, A.A., Carrière, S., Jackson, F., Skuce, P.J.,
831 Rohn, K., and Wolstenholme, A.J. (2009). Molecular detection of benzimidazole resistance in
832 *Haemonchus contortus* using real-time PCR and pyrosequencing. *Parasitology* 136, 349–358.
- 833 Saunders, G.I., Wasmuth, J.D., Beech, R., Laing, R., Hunt, M., Naghra, H., Cotton, J.A., Berriman,
834 M., Britton, C., and Gilleard, J.S. (2013). Characterization and comparative analysis of the
835 complete *Haemonchus contortus* β -tubulin gene family and implications for benzimidazole
836 resistance in strongylid nematodes. *International Journal for Parasitology* 43, 465–475.
- 837 Sheir-Neiss, G., Lai, M.H., and Ronald Morris, N. (1978). Identification of a gene for β -tubulin in
838 *aspergillus nidulans*. *Cell* 15, 639–647.
- 839 Shimko, T.C., and Andersen, E.C. (2014). COPASutils: an R package for reading, processing, and
840 visualizing data from COPAS large-particle flow cytometers. *PLoS One* 9, e111090.
- 841 Silvestre, A., and Cabaret, J. (2002). Mutation in position 167 of isotype 1 beta-tubulin gene of

- 842 Trichostrongylid nematodes: role in benzimidazole resistance? *Mol. Biochem. Parasitol.* *120*, 297–
843 300.
- 844 Stasiuk, S.J., MacNevin, G., Workentine, M.L., Gray, D., Redman, E., Bartley, D., Morrison, A.,
845 Sharma, N., Colwell, D., Ro, D.K., et al. (2019). Similarities and differences in the
846 biotransformation and transcriptomic responses of *Caenorhabditis elegans* and *Haemonchus*
847 *contortus* to five different benzimidazole drugs. *Int. J. Parasitol. Drugs Drug Resist.* *11*, 13–29.
- 848 Sutherland, I.A., and Leathwick, D.M. (2011). Anthelmintic resistance in nematode parasites of
849 cattle: a global issue? *Trends Parasitol.* *27*, 176–181.
- 850 Theodorides, V.J., Scott, G.C., and Lademan, M.S. (1970). Strains of *Haemonchus contortus*
851 resistant against benzimidazole anthelmintics. *Am. J. Vet. Res.* *31*, 859–863.
- 852 Theodorides, V.J., DiCuollo, C.J., Nawalinski, T., Miller, C.R., Murphy, J.R., Freeman, J.F., Killeen,
853 J.C., Jr, and Rapp, W.R. (1977). Toxicologic and teratologic studies of oxibendazole in ruminants
854 and laboratory animals. *Am. J. Vet. Res.* *38*, 809–814.
- 855 van Wyk, J.A., Malan, F.S., and Randles, J.L. (1997). How long before resistance makes it
856 impossible to control some field strains of *Haemonchus contortus* in South Africa with any of the
857 modern anthelmintics? *Vet. Parasitol.* *70*, 111–122.
- 858 Zamanian, M., Cook, D.E., Zdraljevic, S., Brady, S.C., Lee, D., Lee, J., and Andersen, E.C. (2018).
859 Discovery of genomic intervals that underlie nematode responses to benzimidazoles. *PLoS Negl.*
860 *Trop. Dis.* *12*, e0006368.
- 861 Zdraljevic, S., Strand, C., Seidel, H.S., Cook, D.E., Doench, J.G., and Andersen, E.C. (2017).
862 Natural variation in a single amino acid substitution underlies physiological responses to
863 topoisomerase II poisons. *PLoS Genet.* *13*, e1006891.
- 864 Zhao, Y., Long, L., Xu, W., Campbell, R.F., Large, E.E., Greene, J.S., and McGrath, P.T. (2018).
865 Changes to social feeding behaviors are not sufficient for fitness gains of the *Caenorhabditis*
866 *elegans* N2 reference strain. *Elife* *7*.

867

868

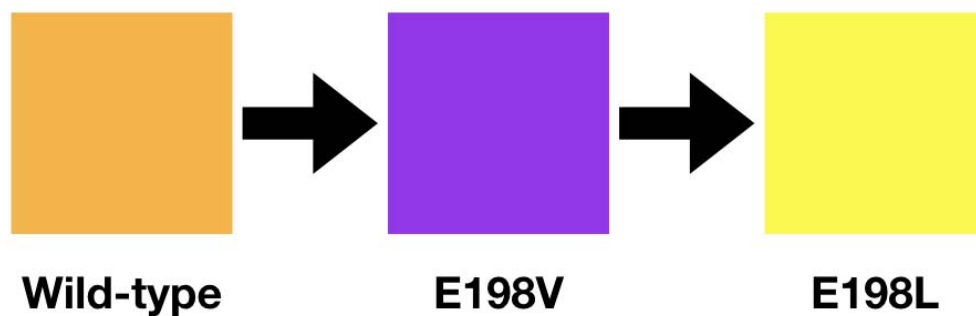
869

870

871

872

873 **Supplemental Figures**



Codon			
198	GAA	GTA	TTA

874

875

876 **Supplemental Figure 1.**

877 Graphical interpretation of the predicted resistance based on allele frequency observations

878 in parasite populations (Avramenko et al., 2019). The boxes at the top represent the

879 strains that are used in this study. The codon at position 198 is shown below and

880 demonstrates how E198V (purple) could be an intermediate one nucleotide step from

881 E198 (orange) to E198L (yellow).

882

883

884

885

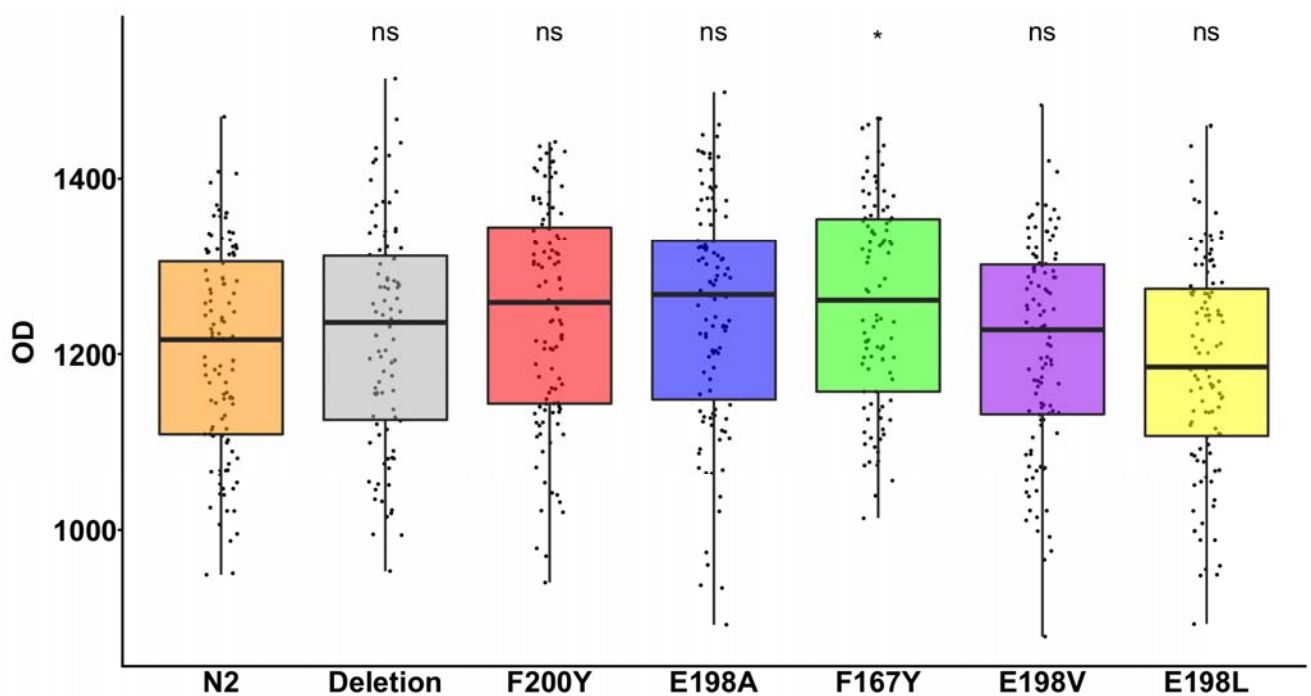
886

887

888

889

890



891

892 **Supplemental Figure 2. Strains containing parasite beta-tubulin alleles in control**
893 **conditions**

894 The x-axis indicates the allele introduced into the N2 strain. Median Optical Densities of
895 populations with the indicated allele in control conditions (DMSO) are plotted on the y-axis.

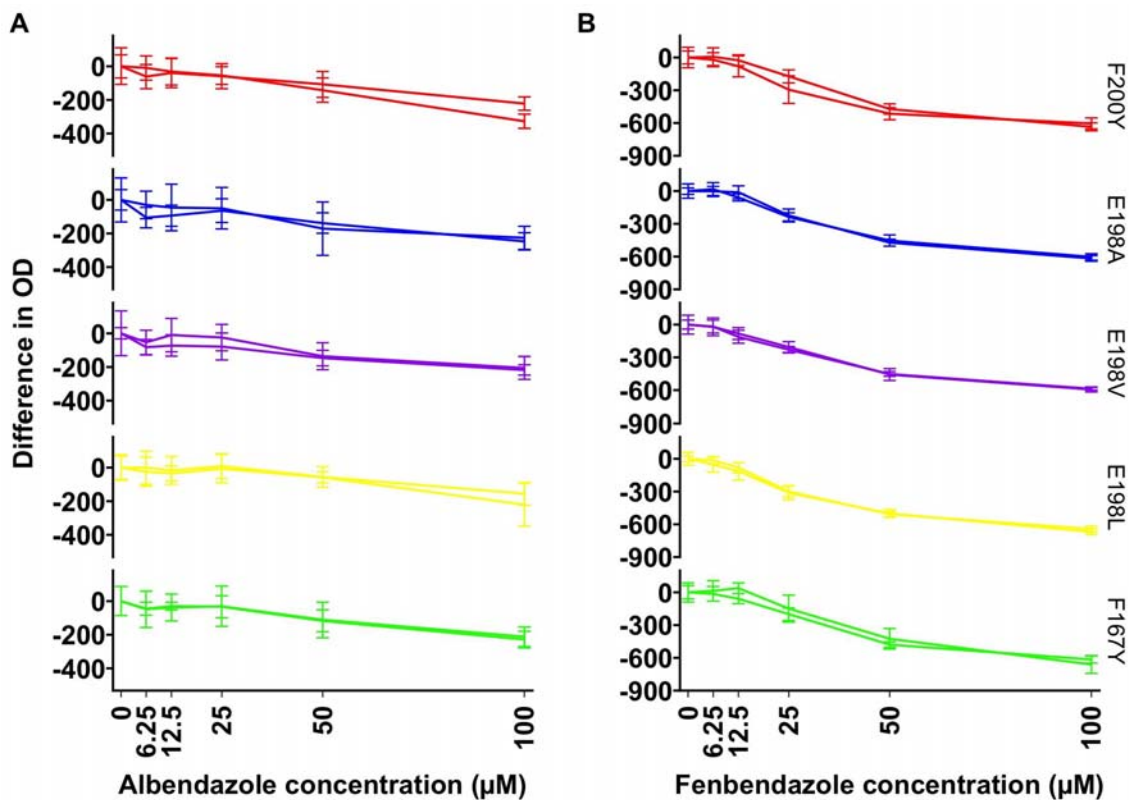
896 Each point represents a population of approximately 35 individuals. The F167Y strain is
897 the only strain significantly different from the N2 strain in control conditions ($p < 0.05$,

898 Tukey HSD).

899

900

901



902

903 **Supplemental Figure 3. Dose-response assays with independently generated alleles**

904 Drug-response assays of both canonical and non-canonical parasite beta-tubulin alleles in
905 (A) albendazole and (B) fenbendazole. Normalized values were calculated by taking the
906 phenotypic trait (median.EXT) value for each population and subtracting the mean
907 median.EXT value of that strain at 0 µM. Normalized trait values are shown in responses
908 to six drug concentrations (0, 6.25, 12.5, 25, 50, and 100 µM) of BZ. Data from two strains
909 with the independent allele replacements are shown for each allele in both albendazole
910 and fenbendazole. The allele replacement is shown to the right of (B) for each row.

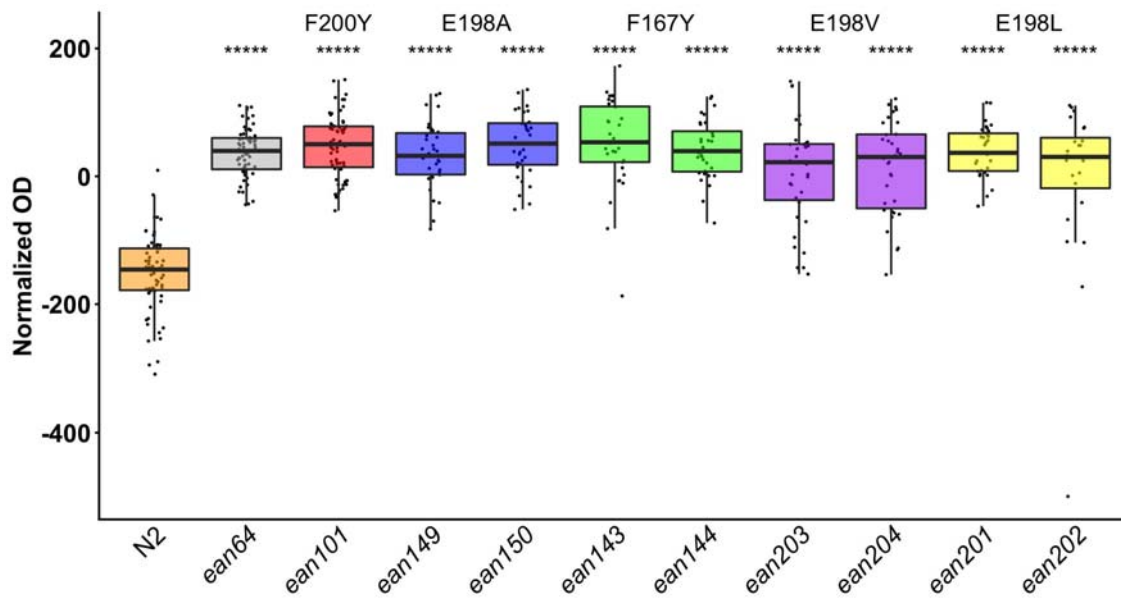
911

912

913

914

915



916

917

918 **Supplemental Figure 4. Independent alleles measured in the high-throughput**
919 **assays at high replication**

920 The x-axis denotes the *ben-1* allele designation of each tested strain (*ean64* = $\Delta ben-1$,
921 *ean101* = F200Y, *ean149* = E198A, *ean150* = E198A, *ean143* = F167Y, *ean144* = F167Y,
922 *ean203* = E198V, *ean204* = E198V, *ean201* = E198L, and *ean202* = E198L). Regressed
923 optical density of response to fenbendazole at 30 μ M. Each point represents a population
924 measurement of approximately 35-50 individuals. Independent edits of the same allele
925 were not statistically different from one another (p-value < 0.0001, Tukey HSD).

926

927

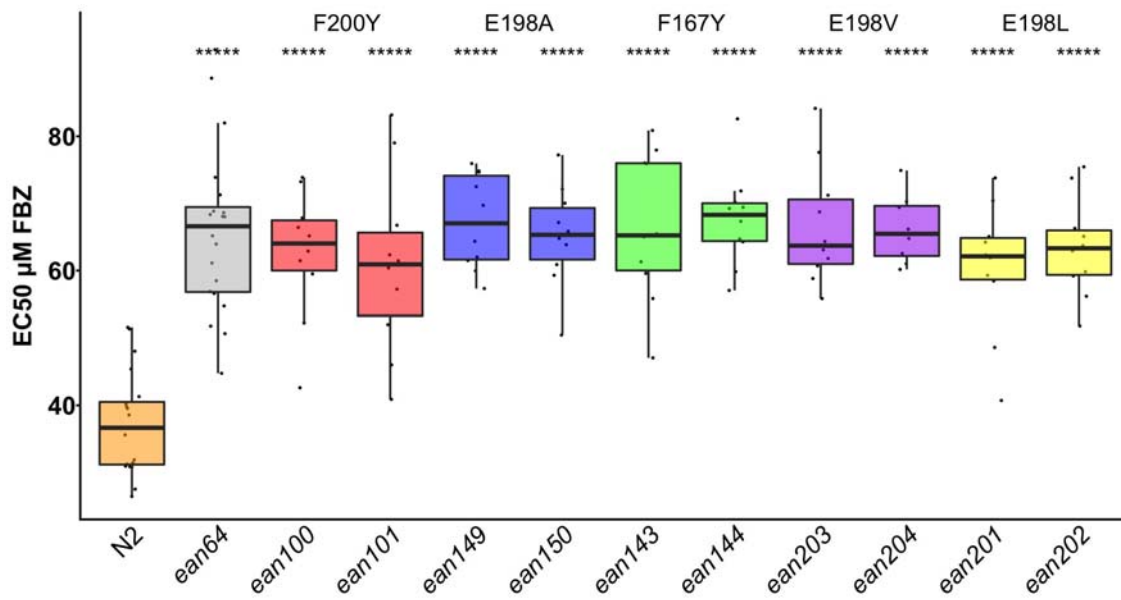
928

929

930

931

932



933

934 **Supplemental figure 5. Estimated fenbendazole EC50 values for each the *ben-1***
935 **edited strains**

936 The x-axis denotes the *ben-1* allele designation of each tested strain (*ean64* = $\Delta ben-1$,
937 *ean100* = F200Y, *ean101* = F200Y, *ean149* = E198A, *ean150* = E198A, *ean143* = F167Y,
938 *ean144* = F167Y, *ean203* = E198V, *ean204* = E198V, *ean201* = E198L, and *ean202* =
939 E198L). The y-axis shows the estimated EC50 in FBZ. Each point represents the
940 estimated EC50 calculated from one replicate of our multi-dose drug assay. A replicate
941 consists of one plate of the assay representing one well of each concentration with 35-50
942 individuals per well. Independent edits of the same allele were not statistically different
943 from one another (p-value > 0.05, Tukey HSD). All alleles had significantly higher EC50
944 calculations than N2 (p-value < 0.0001, Tukey HSD)

945

946

947

948

949

950